# Single leptoquark production at $e^+e^-$ and $\gamma\gamma$ colliders

G. Bélanger and D. London
*Laboratoire de Physique Nucléaire, Université de Montréal, C.P. 6128, Montréal, Québec, Canada H3C 3J7*

H. Nadeau
*Physics Department, McGill University, 3600 University St., Montréal, Québec, Canada H3A 2T8*
(Received 2 August 1993)

We consider single production of leptoquarks (LQ's) at $e^+e^-$ and $\gamma\gamma$ colliders, for two values of the center-of-mass energy: $\sqrt{s}=500$ GeV and 1 TeV. We find that LQ's which couple within the first generation are observable for LQ masses almost up to the kinematic limit, both at $e^+e^-$ and $\gamma\gamma$ colliders, for an LQ coupling strength equal to $\alpha_{\rm em}$. The cross sections for single production of second- and third-generation LQ's at $e^+e^-$ colliders are too small to be observable. In $\gamma\gamma$ collisions, on the other hand, second-generation LQ's with masses much larger than $\sqrt{s}/2$ can be detected. However, third-generation LQ's can be seen at $\gamma\gamma$ colliders only for masses at most $\sim\sqrt{s}/2$, making their observation more probable via the pair production mechanism.

PACS number(s): 14.80.−j, 12.10.Dm, 13.10.+q

One of the more interesting environments in which to study physics beyond the standard model (SM) is at a high-energy linear $e^+e^-$ collider. Not only are $e^+e^-$ collisions clean, but it likely will be possible to adjust the center-of-mass energy. Furthermore, it has been suggested that, by using backscattered laser beams, an $e^+e^-$ machine can be converted into an $e\gamma$ or $\gamma\gamma$ collider [1]. This is particularly exciting, since these different modes may be quite useful for looking for new physics.

Leptoquarks (LQ's), which are absent in the SM but predicted by many of its extensions, are one example of the new physics which can be studied at such machines. LQ's of electromagnetic charge $Q_{\rm em}=-\frac{1}{3}$, $-\frac{2}{3}$, $-\frac{4}{3}$, or $-\frac{5}{3}$ would decay into a charged lepton and a quark or antiquark, so the signal would be quite striking. In principle, LQ's couple to fermions of either helicity. In general, leptoquarks can have spin 0 or 1, but here we concentrate only on scalar LQ's.

Various processes constrain the strength and nature of the LQ couplings to fermions. For example, for LQ's of charge $-\frac{1}{3}$ which couple to both $e^-u$ and $\nu_e d$, rare $\pi$ and $K$ decays constrain the couplings to be chiral [2]. That is, LQ's must couple only to left-handed (LH) or right-handed (RH) quarks, but not both. For these same LQ's, bounds from weak universality require that the LH couplings be at most about 10% of electromagnetic strength. However, these limits need not necessarily apply to leptoquarks of other charges.

One of the most stringent constraints on LQ couplings comes from the absence of low-energy flavor-changing neutral currents (FCNC's). In order to avoid FCNC's, one typically requires the LQ's to couple within a single generation only. However, Leurer [3] has recently pointed out that this requirement is, in fact, impossible to meet in general. Because of Cabibbo-Kobayashi-Maskawa mixing in the left-handed quark sector, one cannot simultaneously diagonalize the couplings of the LQ in both the up-quark and down-quark sector. Thus, if one tries to evade constraints from FCNC's in the down-quark sector, such as $K^0$-$\bar{K}^0$ and $B^0$-$\bar{B}^0$ mixing, by diagonalizing the LH leptoquark couplings, $D^0$-$\bar{D}^0$ mixing will then put very strong limits on the masses and couplings of left-handed LQ's. There are no similar constraints for the right-handed LQ's.

Of course, this should not discourage experimentalists from looking for left-handed LQ's. After all, it is possible that there are other new particles whose effects in low-energy processes would cancel those due to leptoquarks. Thus, if a left-handed LQ were discovered, in fact, *two* types of physics beyond the SM would have been found: the leptoquark itself, and the new physics responsible for the cancellations. This possibility is not totally fantastic, since models which include LQ's will typically also contain other new particles (scalars, gauge bosons, etc.).

In a previous paper [4], two of us investigated the production of scalar leptoquarks at $e\gamma$ colliders at two values of the center-of-mass energy: $\sqrt{s}=500$ GeV and 1 TeV. We showed that LQ's with masses essentially up to the kinematic limit could be seen, even for couplings as weak as $\sim 10^{-3}$–$10^{-2}\alpha_{\rm em}$. In this paper we continue the investigation of single leptoquark production at both $e^+e^-$ and $\gamma\gamma$ colliders, again taking $\sqrt{s}=500$ GeV and 1 TeV. The $e^+e^-$ case was studied some time ago by Hewett and Pakvasa [5], but only for charge $-\frac{1}{3}$ LQ's. Here we do a more extensive analysis.

The most general, model-independent Lagrangian with SU(3)×SU(2)×U(1) invariant couplings of the scalar leptoquarks and conservation of the baryon and lepton numbers [6] can be separated into two pieces:

$$\begin{aligned}\mathcal{L}_L &= g_{1L}\overline{q_L^c}\, i\tau_2 l_L S_1 + g_{3L}\overline{q_L^c}\, i\tau_2 \tau^i l_L S_3^i \\ &\quad + h_{2L}\bar{q}_L i\tau_2 e_R R_2' \,, \\ \mathcal{L}_R &= g_{1R}\overline{u_R^c} e_R S_1' + \tilde{g}_{1R}\overline{d_R^c} e_R \tilde{S}_1 \\ &\quad + h_{2R}\bar{u}_R l_L R_2 + \tilde{h}_{2R}\bar{d}_R l_L \tilde{R}_2 \,.\end{aligned} \tag{1}$$

 

The LH quarks and leptons appear in the standard SU(2) doublets $q_L$ and $l_L$, and the superscript $c$ denotes charge conjugation. In the above equations, following Leurer [3], we have defined the "handedness" of the leptoquarks according to the helicity of the quark or antiquark to which they couple.[1] That is, the LQ's in $\mathcal{L}_L$ and $\mathcal{L}_R$ are left and right handed, respectively. From the above, we see that the LH leptoquarks transform as either a singlet, doublet, or triplet of $SU(2)_W$, while those coupling to RH quarks are singlets or doublets. The $R$ and $S$ leptoquarks carry fermion number 0 and 2, respectively, with their subscript indicating the $SU(2)_W$ multiplet to which they belong.

Despite the rather complicated notation in Eq. (1), for our purposes the only important properties of the leptoquark are its charge and its handedness. It is straightforward to verify that, for each of the four possible electromagnetic charges, there exists a LH and a RH leptoquark. There is one other important point—in all processes of interest in this analysis, only the couplings of the LQ to the charged lepton will enter. We can therefore take the LQ couplings to be generation diagonal. There is no conflict with Leurer's result—there may indeed be a LQ-neutrino-quark (or antiquark) coupling which is not generation diagonal, but this is unimportant here. In summary, then, the leptoquark is defined by its charge, by its handedness, and by the generation of the particles to which it couples. In this paper we will use the symbol $S$ to denote a leptoquark, while $q$ will refer to either a quark or an antiquark.

One advantage of the $\gamma\gamma \to lqS$ process is that it allows for the production of leptoquarks of each of the three generations [7]. As we will see, although second- and third-generation LQ's can indeed be produced in $e^+e^-$ collisions, the cross sections are much too small to be observed.

Let us first focus on single LQ production in $e^+e^-$ collisions. The diagrams which give rise to this are shown in Fig. 1. Although the large number of diagrams may seem daunting, most of these can be neglected. There is a relatively simple way to ascertain which are important and which are not. Consider the diagrams of Fig. 1(a) in which a photon is exchanged. When the virtual photon is aligned with the positron beam direction, the amplitude diverges. This divergence is regulated by the small mass of the positron, giving rise to a logarithmic enhancement of about 30 in the total cross section. In the following, we will refer to such enhancements as "large logs." A quick way to spot diagrams which have large logs is to look for vertices involving three massless (or nearly massless) particles with at least one $t$- or $u$-channel propagator. Application of this rule reveals that none of the diagrams in Figs. 1(b) or 1(c) have large logs, so these diagrams can be neglected, and similarly for those diagrams in Fig. 1(a) in which a $Z$ is exchanged. In fact, with this

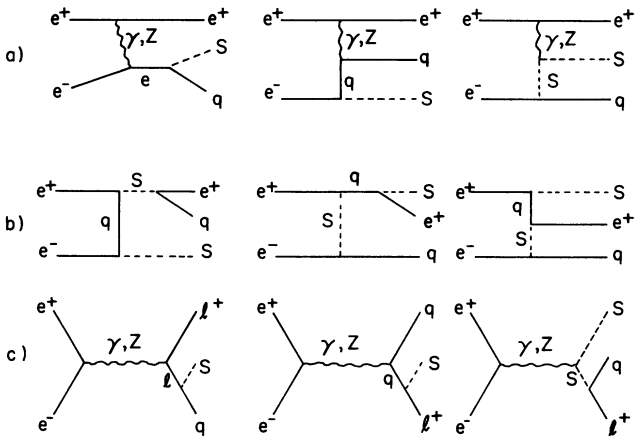


FIG. 1. The three sets of diagrams contributing to the process $e^+e^- \to e^+qS$. $q$ represents either a quark or an antiquark.

rule one expects that the second diagram of Fig. 1(a) with photon exchange should have an additional large log due to the quark propagator. We will see below that this is indeed the case.

The presence of these divergences indicates that most of the cross section comes from a few directions in phase space. This makes it very difficult to use conventional Monte Carlo methods for computing phase-space integrals. A much simpler way to evaluate the diagrams of Fig. 1(a) in which a photon is exchanged is to use the effective photon approximation [8]:

$$\sigma(s)=\int_{s_{\rm th}/s}^{1} d\tau f_\gamma(\tau)\hat{\sigma}(\tau s)\ , \tag{2}$$

in which $\sigma(s)$ is the cross section for the process $e^+e^- \to e^+qS$ at a center-of-mass energy $s$, and $\hat{\sigma}(\tau s)$ is the cross section for the subprocess $\gamma e^- \to qS$ with a center-of-mass energy $\hat{s}=\tau s$. The minimum $\hat{s}$ required $(s_{\rm th})$ is $(M_S+m_q)^2$. The photon distribution function $f_\gamma(\tau)$ is [8]

$$f_\gamma(\tau)=\frac{\alpha}{2\pi}\left[\frac{1+(1-\tau)^2}{\tau}\ln\left[\frac{s}{4m_e^2}\frac{1-2\tau+\tau^2}{1-\tau+\tau^2/4}\right]+\tau\ln\left[\frac{2-\tau}{\tau}\right]+\frac{2(\tau-1)}{\tau}\right]. \tag{3}$$

As expected, $f_\gamma(\tau)$ contains a large log. Note that the more common form of this function,

$$f_\gamma(\tau)=\left[\frac{\alpha}{2\pi}\ln\frac{s}{4m_e^2}\right]\frac{1+(1-\tau)^2}{\tau}\ , \tag{4}$$

is quite adequate when $M_S$ is relatively small compared to $\sqrt{s}$. However, for large $M_S$ the full form [Eq. (3)] must be used.

In order to use Eq. (2), we must evaluate the cross section for $\gamma e^- \to qS$. The diagrams describing this process are shown in Fig. 2. The key point which must be addressed is that, in the limit in which the quark mass is neglected, the second diagram diverges. This corresponds to the situation in which the photon and the

[1]Note that this differs from the conventions of Ref. [4], in which the handedness of the LQ is defined by the helicity of the lepton.

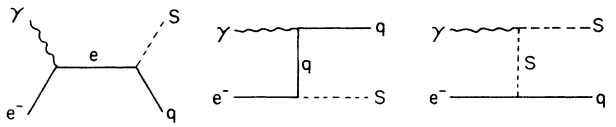


FIG. 2. Diagrams contributing to the process $\gamma e^- \to qS$. $q$ represents either a quark or an antiquark.

quark are aligned. One way to deal with this is to impose a $p_T$ cut on the quark jet [5]. The problem with this solution is that, because the large logs are due to that region of phase space in which the entire event is collinear, one loses a considerable fraction of the total cross section. An alternative procedure, which is the one we advocate, is to use the nonzero quark mass as a regulator. As we will see, this results in a significant enhancement of the total cross section compared to the $p_T$ cut. Experimentally, the situation is that the entire event goes down the beam pipe. However, the leptoquark will then decay into a jet and a lepton, giving a signal in the detector which is unmistakable: $\gamma e^-$ (or $e^+e^- \to e^-$ + jet. For comparison, we will present both methods of regulating the divergence.

We first consider calculating the diagrams of Fig. 2 neglecting the lepton mass, but keeping a nonzero mass for the quark, $m_q$. For all leptoquarks we will use the generic Yukawa coupling constant $g$, with the understanding that the coupling could depend on the masses involved and might vary from one generation to the other. We parametrize the strength of the LQ coupling by comparing it to the electromagnetic interaction, i.e., $g^2 = 4\pi k \alpha_{\rm em}$, and allowing $k$ to vary. Denoting the charge of the leptoquark by $Q_S$, the full expression for $\hat{\sigma}(s)$ is then found to be

$$\hat{\sigma}(\hat{s}) = \frac{\pi k \alpha_{\rm em}^2}{2\hat{s}} \left\{ \left[ 2 + 2Q_S(2Q_S+1) - 4Q_S(Q_S+1)\alpha - \frac{7}{2}\alpha \right] \beta \right.$$
$$+ (Q_S+1) \left[ (Q_S+1)(1-2\alpha+2\alpha^2) + 4Q_S(1-\alpha)\frac{m_q^2}{\hat{s}} \right] \ln\left[ \frac{\alpha+\beta}{\alpha-\beta} \right]$$
$$\left. + 2Q_S(1-\alpha) \left[ -2\frac{M_S^2}{\hat{s}} + Q_S \left[ \alpha - 2\frac{m_q^2}{\hat{s}} \right] \right] \ln\left[ \frac{2-\alpha-\beta}{2-\alpha+\beta} \right] \right\} \quad (5)$$

in which

$$\alpha \equiv 1 - \frac{M_S^2 - m_q^2}{\hat{s}} \quad (6)$$

and

$$\beta \equiv \left[ 1 - 2\frac{M_S^2 + m_q^2}{\hat{s}} + \frac{(M_S^2 - m_q^2)^2}{\hat{s}^2} \right]^{1/2} . \quad (7)$$

One important point to notice is that Eq. (5) is independent of the handedness of the LQ. In other words, the cross section for the subprocess $\gamma e^- \to qS$ is the same for both LH and RH leptoquarks of charge $Q_S$.

The cross section for single leptoquark production in the process $e^+e^- \to e^+qS$ can now be calculated using the effective photon approximation by substituting Eq. (5) into Eq. (2) and numerically computing the integral. Our results for $\sqrt{s} = 500$ GeV and 1 TeV appear in Figs. 3(a) and 3(b), where we have taken the LQ coupling strength to be equal to that of the electromagnetic interaction, i.e., $k = 1$, and have set $m_q = 7$ MeV (this corresponds roughly to either a $d$- or $u$-quark mass). Assuming the integrated luminosity at a high-energy $e^+e^-$ collider to be 10 fb$^{-1}$ at 500 GeV, and 60 fb$^{-1}$ at 1 TeV, and requiring 25 events for discovery, one can see that LQ's almost up to the kinematic limit can be seen in $e^+e^-$ colliders. More precisely, LQ's with $Q_S = -\frac{1}{3}$ and $-\frac{5}{3}$ are observable if $M_S \leq 475$ GeV (960 GeV) at $\sqrt{s} = 500$ GeV (1 TeV), and those with $Q_S = -\frac{2}{3}$ and $-\frac{4}{3}$ can be seen for $M_S \leq 420$ GeV (870 GeV) at $\sqrt{s} = 500$ GeV (1 TeV). These numbers are given explicitly in Table I, where they can be compared with the prospects at $\gamma\gamma$ colliders, which we will discuss later in the paper. Since the cross section is linear in $k$, it is straightforward to scale the results shown in Fig. 3 to other values of $k$, if desired. It should also be stressed that, because we have used an approximation in the calculation, there is some uncertainty in the above numbers, perhaps as much as 5% [9].

Note that all cross sections in this paper are calculated for the processes $e^+e^- \to e^+qS$ and $\gamma\gamma \to l^+qS$. The conjugate processes $e^+e^- \to e^-\bar{q}\bar{S}$ and $\gamma\gamma \to l^-\bar{q}\bar{S}$ have identical rates. Furthermore, following the conventions of the literature, we have not included in our cross-section calculations the additional factor of 3 due to the three colors of LQ. Therefore, if one wishes to consider both $S$ and $\bar{S}$ production, and to take into account the three colors, our cross sections should, in practice, be multiplied by a factor of 6.

As pointed out above, most of the cross section comes from that region of phase space in which the entire event goes down the beam pipe. Since the LQ decays to $l$ + jet, there will essentially be no background from SM processes. Even for those events in which other particles are seen in the detector, there will be a sharp invariant mass peak in $M_{l+\rm jet}$ at $M_S$, which is not present in SM decays.

One interesting feature of Fig. 3 is that the cross sections for the LQ's with $Q_S = -\frac{1}{3}$ and $-\frac{5}{3}$ are almost equal, and similarly for those LQ's with $Q_S = -\frac{2}{3}$ and $-\frac{4}{3}$. This reflects the dominance of the second diagram in Fig. 2, since it has an extra large log compared to the other two. Since the amplitude for this diagram is pro-

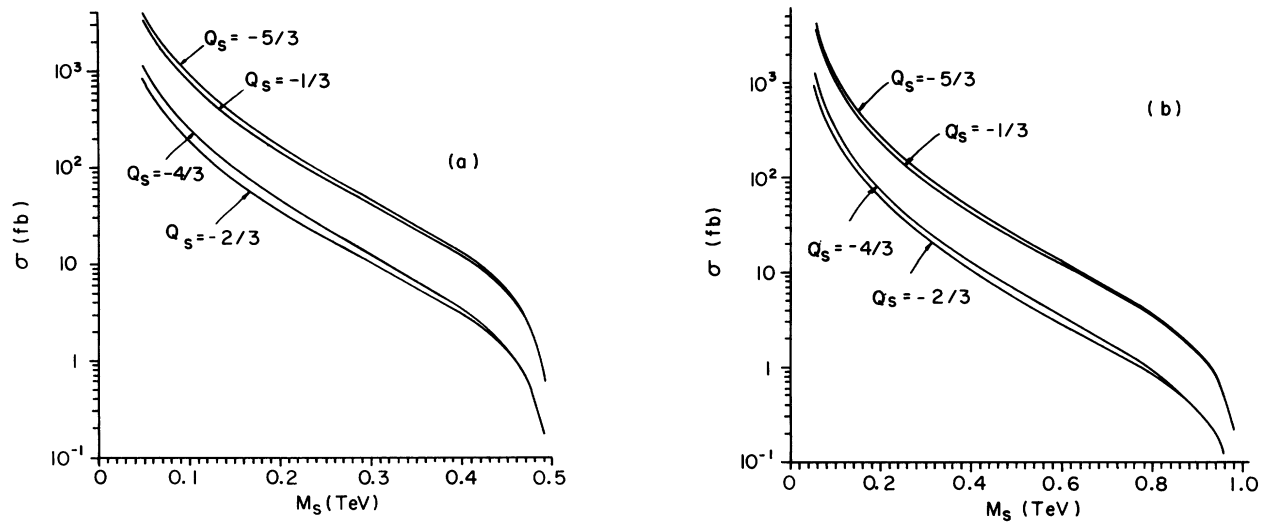


FIG. 3. Cross sections for single leptoquark production in $e^+e^-$ collisions at (a) $\sqrt{s}=500$ GeV, (b) $\sqrt{s}=1$ TeV for the four possible LQ charges, $Q_S=-\frac{1}{3}, -\frac{2}{3}, -\frac{4}{3}$, and $-\frac{5}{3}$. The results are given for $k=1$. Here we have used the nonzero quark mass as a regulator (see text).

portional to the quark charge, $Q_q=-(Q_S+1)$, the most important term in $\hat{\sigma}(\hat{s})$ is the one whose coefficient is $(Q_S+1)^2$. From this it follows that, to a very good approximation, the cross sections for LQ's with $Q_S=-\frac{1}{3}$ and $-\frac{5}{3}$ should be equal. Similarly, LQ's with $Q_S=-\frac{2}{3}$ and $-\frac{4}{3}$ are expected to have equal cross sections, and these should be a factor of 4 smaller than the cross section for the LQ with $Q_S=-\frac{1}{3}$. These expectations are born out in Fig. 3.

We have also calculated the diagrams in Fig. 2 by imposing a $p_T$ cut on the quark jet. In this case, the cross section for $\gamma e^- \to qS$ takes the form

$$\hat{\sigma}(\hat{s})=\frac{\pi k\alpha_{\rm em}^2}{2\hat{s}^2}\left\{-\frac{1}{2\hat{s}}(u_{\max}^2-u_{\min}^2)+2\left[\frac{M_S^2}{\hat{s}}-(Q_S+1)\right](u_{\max}-u_{\min})-2Q_S^2M_S^4\left[\frac{1}{\hat{s}+u_{\max}}-\frac{1}{\hat{s}+u_{\min}}\right]\right.$$
$$\left.+(Q_S+1)^2\left[\hat{s}-2M_S^2+\frac{2M_S^4}{\hat{s}}\right]\ln\left[\frac{u_{\min}}{u_{\max}}\right]+2Q_SM_S^2\left[-2\frac{M_S^2}{\hat{s}}+Q_S\left[1-\frac{M_S^2}{\hat{s}}\right]\right]\ln\left[\frac{\hat{s}+u_{\min}}{\hat{s}+u_{\max}}\right]\right\}. \quad (8)$$

TABLE I. The largest LQ mass (in GeV) observable, for each of the four LQ charges and for each of the three generations, in the processes $e^+e^-\to e^+qS$ and $\gamma\gamma\to l^+qS$ at (a) $\sqrt{s}=500$ GeV and (b) $\sqrt{s}=1$ TeV. Second- and third-generation LQ's cannot be seen at $e^+e^-$ colliders.

| | $Q_S$ | (a) $(M_S)_{\max}$ | (b) $(M_S)_{\max}$ |
|---|---|---|---|
| | $e^+e^-\to e^+qS$ | | |
| First generation | $-\frac{1}{3}, -\frac{5}{3}$ | 475 | 960 |
| | $-\frac{2}{3}, -\frac{4}{3}$ | 420 | 870 |
| | $\gamma\gamma\to l^+qS$: | | |
| First generation | $-\frac{1}{3}, -\frac{5}{3}$ | 480 | 970 |
| | $-\frac{2}{3}, -\frac{4}{3}$ | 425 | 920 |
| Second generation | $-\frac{1}{3}$ | 400 | 900 |
| | $-\frac{5}{3}$ | 420 | 910 |
| | $-\frac{2}{3}$ | 280 | 720 |
| | $-\frac{4}{3}$ | 320 | 780 |
| Third generation | $-\frac{1}{3}$ | | 180 |
| | $-\frac{5}{3}$ | 140 | 530 |
| | $-\frac{2}{3}$ | 100 | 400 |
| | $-\frac{4}{3}$ | 190 | 540 |

Here

$$u_{\max}=-\tfrac{1}{2}\hat{s}\beta'(1-c_{\max}),\quad u_{\min}=-\tfrac{1}{2}\hat{s}\beta'(1+c_{\max}),\qquad (9)$$

with

$$\beta'=1-\frac{M_S^2}{\hat{s}},\quad c_{\max}=\left[1-\frac{4p_{T\text{cut}}^2}{\hat{s}(\beta')^2}\right]^{1/2},\qquad (10)$$

in which $p_{T\text{cut}}$ is the imposed $p_T$ cut which we take to be 10 GeV.

Note that, although the two different methods of regulating the collinear divergence appear to give very different expressions for the total cross section, Eqs. (5) and (8) are, in fact, quite similar. If one replaces $p_{T\text{cut}}$ in Eq. (8) by $m_q$, then the two expressions are identical to lowest order in $m_q^2$, apart from the single finite term

$$(\pi k\alpha_{\text{em}}^2/2\hat{s}^2)[2\beta' M_S^2(Q_S+1)^2]\ .$$

We now calculate as before the cross section for single leptoquark production in the process $e^+e^-\to e^+qS$ using the $\hat{\sigma}(\hat{s})$ given in Eq. (8). For simplicity we consider $Q_S=-\frac{1}{3}$ LQ's only, taking $k=1$ and $\sqrt{s}=1$ TeV. The result is shown in Fig. 4. Comparing Figs. 3(b) and 4, we see that the rates shown in Fig. 4 are a factor 4–5 smaller than those in Fig. 3(b) (for $Q_S=-\frac{1}{3}$) for the same LQ mass. In other words, one gains a significant amount in the total cross section for single leptoquark production by *not* imposing a $p_T$ cut, but rather using the nonzero quark mass to regulate the collinear divergence. Furthermore, as discussed earlier, the experimental signal is quite striking using this method. For the rest of the paper, we will restrict ourselves to evaluating the large logs using a nonzero quark mass.

Since we have assumed that each LQ couples generation diagonally, the production cross section shown in Fig. 3 hold only for first generation leptoquarks. The only way to produce single second- or third-generation LQ's in $e^+e^-$ collisions is through the graphs of Fig. 1(c). Note, however, that there are no large logs in these diagrams, so we expect the cross sections to be smaller than those of Fig. 3 by at least two to three orders of magnitude. We have calculated these diagrams explicitly, and we find that indeed the single LQ production cross sections are typically $\sim 10^{-3}$ fb. Thus, there is no hope for seeing single second- or third-generation LQ's in $e^+e^-$ collisions.[2] It is, however, possible to observe such LQ's in $\gamma\gamma$ collisions, and we now turn to a study of such processes.

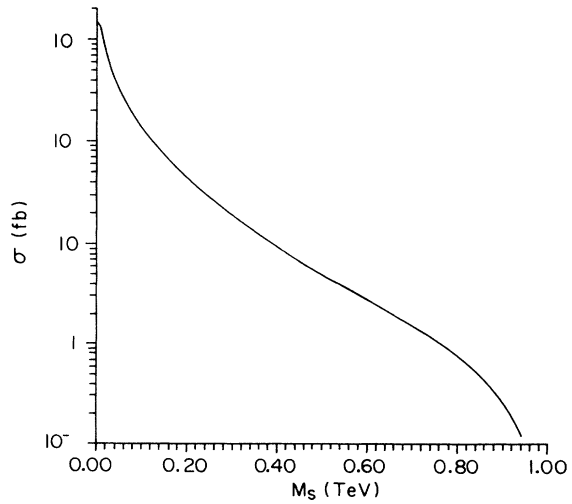


FIG. 4. Cross section for single leptoquark production in $e^+e^-$ collisions at $\sqrt{s}=1$ TeV, using $Q_S=-\frac{1}{3}$ and $k=1$. Here we have used a 10 GeV $p_T$ cut as a regulator (see text).

For the process $\gamma\gamma\to l^+qS$, there are six diagrams, shown in Fig. 5. In fact, there are really twelve diagrams, since each final state must be symmetrized with respect to the initial photons. Again, it is not necessary to calculate all the graphs—some can be neglected. Using the large log counting rules introduced earlier, one finds that, for the case in which the quark mass is small, the diagram in Fig. 5(a) contains two large logs, the four diagrams of Figs. 5(b) and 5(c) each have one large log, while the diagram in Fig. 5(d) has none. Our experience with single LQ production in $e^+e^-$ collisions tells us that the graph in Fig. 5(a) will essentially completely dominate in this case. For third-generation LQ's, the mass of the top quark ($\sim 150$ GeV) can no longer be considered small compared to the center-of-mass energy. In this case, the large log counting changes—the graphs in Figs. 5(a) and 5(b) each have one large log, while those in Figs. 5(c) and 5(d) have none. Therefore, for LQ's of all generations, it is an excellent approximation to keep only the diagrams

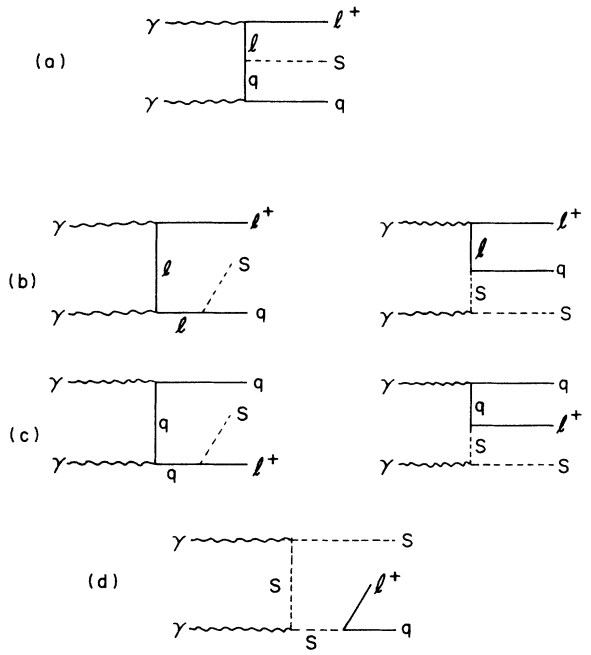


FIG. 5. The four sets of diagrams contributing to the process $\gamma\gamma\to l^+qS$. $q$ represents either a quark or an antiquark.

[2]Note that second- and third-generation LQ's could be seen if they were pair produced in $e^+e^-$ collisions via $s$-channel $\gamma$ or $Z$ exchange. Of course, this is only possible for $M_S\le\sqrt{s}/2$.

in Figs. 5(a) and 5(b) in the calculation of the total cross section, and this is what we will do.

Note that, although we must include the interference among the three diagrams of Figs. 5(a) and 5(b) in our calculation, we may ignore the interference between this set of three graphs and the set which is symmetrized with respect to the initial photons. This can be seen intuitively as follows. The divergences in one set of graphs, which give rise to the large logs, occur when the virtual lepton goes in the direction of the one of the initial photons, while the divergences of other set of graphs are present in that region of phase space in which the virtual lepton aligns itself with the other photon. Therefore, when these two sets of graphs interfere, there are no divergences, and hence no large logs. We have verified this intuitive picture analytically, and find that indeed there are no large logs coming from the interference of the two sets of diagrams. Thus, it is only necessary to evaluate the contribution of the graphs of Figs. 5(a) and 5(b) to the process $\gamma\gamma\to l^+qS$, and then to include a factor of 2 to take into account the symmetrized set of diagrams.

The easiest way to calculate the diagrams in Figs. 5(a) and 5(b) is to use a technique similar to that used in the computation of $e^+e^-\to e^+qS$, namely, the effective fermion approximation. That is,

$$\sigma(s)=\int_{s_{\rm th}/s}^{1} d\tau f_l(\tau)\hat{\sigma}(\tau s)\ , \tag{11}$$

in which $\sigma(s)$ is the cross section for $\gamma\gamma\to l^+qS$ at center-of-mass energy $s$, and $\hat{\sigma}(\tau s)$ is the cross section for the subprocess $\gamma l^-\to qS$ with center-of-mass energy $\hat{s}=\tau s$, just as in the effective photon approximation. The lepton distribution function is [9]

$$f_l(\tau)=\frac{\alpha}{2\pi}\left[[\tau^2+(1-\tau)^2]\ln\left[\frac{s}{4m_l^2}(1-\tau)^2\right]+2\tau(1-\tau)\right]\ . \tag{12}$$

Again, as expected, this function contains a large log. Although $f_l(\tau)$ somewhat resembles the photon distribution function $f_\gamma(\tau)$ [Eq. (3)], there is one important difference. Because of the absence of a factor of $\tau$ in the denominator, $f_l(\tau)$ is much smoother than $f_\gamma(\tau)$. Thus we do not expect the cross section for $\gamma\gamma\to l^+qS$ to be as strong a function of $M_S$ as we found in $e^+e^-\to e^+qS$.

The cross section for the subprocess $\gamma l^-\to qS$ has already been calculated [Eqs. (5)–(7)], so we can simply perform the numerical integration of Eq. (11) for all three generations. We have taken $m_e=0.5$ MeV and $m_u=m_d=7$ MeV for the first generation, $m_\mu=100$ MeV, $m_s=150$ MeV and $m_c=1.5$ GeV for the second, and $m_\tau=1.5$ GeV, $m_b=5$ GeV, and $m_t=150$ GeV for the third. We remind the reader that the LQ's of charge $-\frac{1}{3}$ and $-\frac{5}{3}$ couple to up-type quarks, while the $Q_{\rm em}=-\frac{2}{3}$ and $-\frac{4}{3}$ LQ's couple to down-type quarks. In computing the cross section, we have included the factor 2 to take into account the symmetrized set of diagrams.

The results are shown in Fig. 6 for the three generations, for $\sqrt{s}=500$ GeV and 1 TeV, for $k=1$. Before describing the results, let us note some general features. For the first- and second-generation LQ's, the similarity of the curves for LQ's of $Q_{\rm em}=-\frac{1}{3}$ and $-\frac{5}{3}$ and for LQ's with charges $-\frac{2}{3}$ and $-\frac{4}{3}$, again reflects the dominance of the diagram in Fig. 5(a) (two large logs). Also, as expected, the cross sections are, in general, less strongly dependent on the LQ mass than was found in $e^+e^-$ colliders. Finally, the cross sections for third-generation LQ's are significantly smaller than for those coupling within the first and the second generations. This reflects the fact that there is really one less large log in the cross section for third-generation LQ's.

The figure of merit in Fig. 6 is the largest LQ mass observable for each of the three generations. The question is this: which has the better prospects for LQ detection, the single LQ production mode, or the pair production mode (in which LQ's of mass $M_S\le\sqrt{s}/2$ can be seen)? Looking at Fig. 6, if LQ's of mass greater than $\sqrt{s}/2$ can be seen, then it is better to try to detect leptoquarks in the single LQ production mode. However, if the maximum LQ mass which can be observed is less than $\sqrt{s}/2$, then pair production is more promising. In Table I we display $(M_S)_{\rm max}$ for all four LQ charges and for all three generations.

From Figs. 6(a) and 6(b) and Table I, we see that, as in $e^+e^-$ colliders, first-generation LQ's with masses almost up to the kinematic limit can be seen in $\gamma\gamma\to l^+qS$. As before, we have assumed an integrated luminosity of 10 fb$^{-1}$ at 500 GeV, and 60 fb$^{-1}$ at 1 TeV, and assumed a discovery signal of 25 events. And again, there is perhaps a 5% uncertainty in these numbers due to the approximations used [9].

The situation is similar, though not quite as promising, for second-generation LQ's [Figs. 6(c) and 6(d) Table I]. At $\sqrt{s}=500$ GeV, the maximum mass allowed for observing a LQ is about 300–400 GeV, depending on the LQ charge, while at 1 TeV, it is 700–900 GeV. We remind the reader that we have used the $c$-quark mass in the cross sections for LQ's with charge $-\frac{1}{3}$ and $-\frac{5}{3}$, and the $s$-quark mass for LQ's with $Q_{\rm em}=-\frac{2}{3}$ and $-\frac{4}{3}$.

Things are very different for third-generation LQ's [Figs. 6(e) and 6(f), Table I]. At $\sqrt{s}=500$ GeV, the maximum mass is 100–200 GeV, except for the charge $-\frac{1}{3}$ LQ, which is not observable at all. At 1 TeV, $(M_S)_{\rm max}$ is 180–540 GeV. For third generation leptoquarks, then, it is almost always better to look for pair production in $e^+e^-$ or $\gamma\gamma$ collisions. It should be emphasized, however, that these cross sections have been calculated for LQ coupling strengths $k=1$. If the LQ couplings were proportional to masses, then for those LQ's which couple to the $t$ quark one might conceivably have $k$ larger than one, and the cross sections would increase accordingly. Of course, if $k$ were much larger than one, then at some point this perturbative analysis would break down.

An important point to remember is that, in $\gamma\gamma$ colliders created by the backscattering of laser light, the photon beams are not monochromatic. For a complete calculation it would be necessary to fold in the energy spectrum of the initial photons. Typically the highest-energy photons would have about 80% of the energy of the

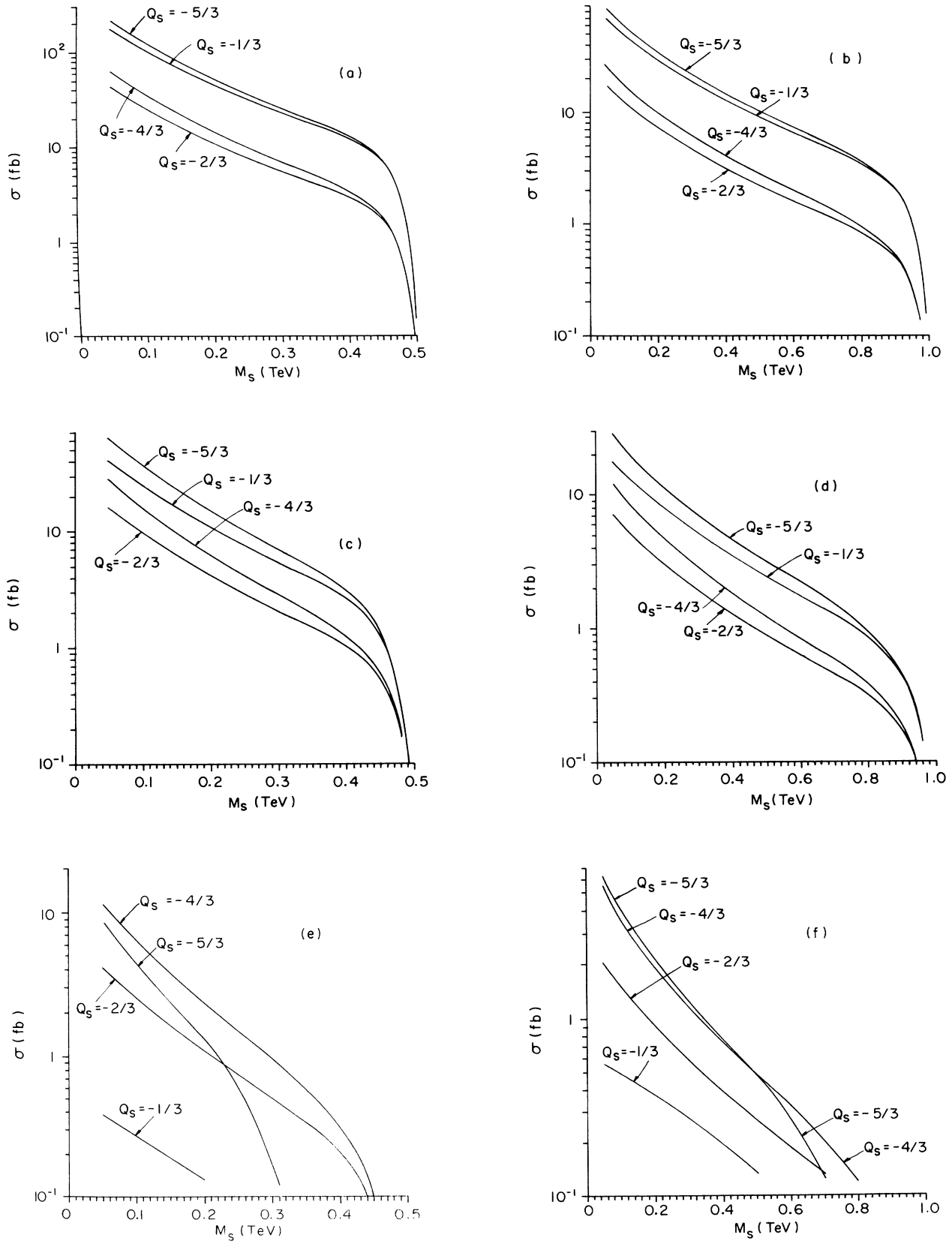


FIG. 6. Cross sections for single leptoquark production in $\gamma\gamma$ collisions for the four possible LQ charges, $Q_s = -\frac{1}{3}, -\frac{2}{3}, -\frac{4}{3}$, and $-\frac{5}{3}$, for (a) first-generation LQ's at $\sqrt{s} = 500$ GeV, (b) first-generation LQ's at $\sqrt{s} = 1$ TeV, (c) second-generation LQ's at $\sqrt{s} = 500$ GeV, (d) second-generation LQ's at $\sqrt{s} = 1$ TeV, (e) third-generation LQ's at $\sqrt{s} = 500$ GeV, (f) third-generation LQ's at $\sqrt{s} = 1$ TeV. The results are given for $k = 1$.

parent electron machine so that the limits given in Table I would be scaled accordingly.

In conclusion, we have calculated the cross sections for single leptoquark production at high-energy $e^+e^-$ and $\gamma\gamma$ colliders of $\sqrt{s}=500$ GeV and 1 TeV. For LQ's coupling within each of the first, second, and third generations, we have considered the four LQ charges $Q_S=-\frac{1}{3}$, $-\frac{2}{3}$, $-\frac{4}{3}$, and $-\frac{5}{3}$. Our results are independent of whether the LQ couples to left- or right-handed quarks or antiquarks.

For the process $e^+e^-\to e^+qS$ we have utilized the effective photon approximation, while for $\gamma\gamma\to l^+qS$ the effective fermion approximation was used. For each of these methods it was necessary to calculate the cross section for the subprocess $\gamma l^-\to qS$. We have shown that using a $p_T$ cut to regulate the collinear divergence in this process is, in fact, not optimal procedure—one loses too much of the total cross section. It is better to use the nonzero quark mass as a regulator. In this case the bulk of the cross section comes from that region of phase space in which the entire event goes down the beam pipe. When the LQ decays, this results in an unmistakable signal in the detector: $e^+e^-$ (or $\gamma\gamma$)$\to l^-$+jet. This is virtually background-free.

We have found that first-generation LQ's of any charge can be observed almost up to the kinematic limit in both $e^+e^-$ and $\gamma\gamma$ colliders ($\sqrt{s}=500$ GeV or 1 TeV) for LQ coupling strengths equal to that of the electromagnetic interaction. For second- and third-generation leptoquarks, the cross sections for single LQ production at $e^+e^-$ colliders are too small to be observable. These LQ's can, however, be seen at $\gamma\gamma$ colliders. Depending on their charges, second-generation leptoquarks with masses between 700 and 900 GeV can be observed in $\gamma\gamma$ collisions at $\sqrt{s}=1$ TeV, while at 500 GeV machines, LQ's whose mass is roughly between 300 and 400 GeV are detectable. For third-generation leptoquarks, the situation is not nearly as promising. At $\sqrt{s}=500$ GeV, only LQ's with masses of at most 190 GeV are observable, while at 1 TeV, it is possible to see LQ's with $M_S$ up to just over 500 GeV. Thus, for third-generation leptoquarks, it seems that it is just as good, if not better, to look for signals from pair production. Of course, if the LQ coupling strength were significantly stronger than $\alpha_{\rm em}$, as might be the case where the top quark is involved, then single third-generation LQ production would become more promising.

We would like to thank I. F. Ginzburg and J. L. Hewett for helpful conversations. This work was supported in part by the Natural Sciences and Engineering Research Council of Canada, and by Fonds pour la Formation de Chercheurs et l'aide à la Recherche, Québec.

[1] I. F. Ginzburg, G. L. Kotkin, V. G. Serbo, and V. I. Telnov, Pis'ma Zh. Eksp. Teor. Fiz. **34**, 514 (1981) [JETP Lett. **34**, 491 (1981)]; Yad. Fiz. **38**, 372 (1983) [Sov. J. Nucl. Phys. **38**, 222 (1983)]; Nucl. Instrum. Methods **205**, 47 (1983); I. F. Ginzburg, G. L. Kotkin, S. L. Panfil, V. G. Serbo, and V. I. Telnov, Yad. Fiz. **38**, 1021 (1983) [Sov. J. Nucl. Phys. **38**, 614 (1983)]; Nucl. Instrum. Methods **219**, 5 (1984).

[2] W. Buchmüller and D. Wyler, Phys. Lett. B **177**, 377 (1986).

[3] M. Leurer, Phys. Rev. Lett. **71**, 1324 (1993).

[4] H. Nadeau and D. London, Phys. Rev. D **47**, 3742 (1993). For another discussion of single scalar LQ production in $e\gamma$ colliders, see O. J. P. Éboli *et al.*, Phys. Lett. B **311**, 147 (1993).

[5] J. L. Hewett and S. Pakvasa, Phys. Lett. B **227**, 178 (1989).

[6] W. Buchmüller, R. Rückl, and D. Wyler, Phys. Lett. B **191**, 422 (1987).

[7] I. F. Ginzburg, in *Proceedings of the IX International Workshop on Photon-Photon Collisions,* edited by D. Caldwell and H. Paar (World Scientific, Singapore, 1993), p. 474.

[8] V. M. Budnev, I. F. Ginzburg, G. V. Meledin, and V. G. Serbo, Phys. Rep. C **15**, 182 (1975).

[9] I. F. Ginzburg and V. G. Serbo, "The $\gamma\gamma\to Zl^+l^-$ and $\gamma\gamma\to Zq\bar{q}$ processes at the polarized photon beams," Novosibirsk report (unpublished); see also P. Kessler, Nuovo Cimento **17**, 809 (1960); V. M. Baier, V. S. Fadin, and V. A. Khoze, Nucl. Phys. **B65**, 381 (1973).